

UV-LED/P25-based photocatalysis for effective degradation of isothiazolone biocide

Xinzheng Li¹, Zhiming Li¹, Zhihui Xing¹, Zhimin Song¹, Bei Ye², Zhengming Wang (✉)³, Qianyuan Wu (✉)¹

¹ Key Laboratory of Microorganism Application and Risk Control of Shenzhen, Guangdong Provincial Engineering Research Center for Urban Water Recycling and Environmental Safety, International Graduate School at Shenzhen, Tsinghua University, Shenzhen 518055, China

² China Shenzhen Environmental Science and New Energy Technology Engineering Laboratory, Tsinghua-Berkeley Shenzhen Institute, Shenzhen 518055, China

³ Environmental Management Research Institute, National Institute of Advanced Industrial Science and Technology, 16-1 Onogawa, Tsukuba, Ibaraki, 305-8569, Japan

HIGHLIGHTS

- UV-LED with shorter wavelength was beneficial for photocatalytic degradation.
- SRNOM dramatically inhibit the degradation.
- $\cdot\text{OH}$ acts as the active radical in photocatalytic degradation.
- Degradation mainly undergoes oxidation, hydrolysis and chain growth reactions.

ARTICLE INFO

Article history:

Received 6 August 2020

Revised 23 September 2020

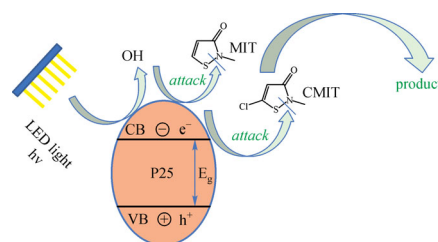
Accepted 7 October 2020

Available online 10 December 2020

Keywords:

Degradation
Photocatalytic
LED
CMIT
P25

GRAPHIC ABSTRACT



ABSTRACT

In this work, LED-based photocatalysis using mixed rutile and anatase phase TiO_2 (P25) as the photocatalyst could effectively remove 5-chloro-2-methyl-4-isothiazolin-3-one (CMIT) and methylisothiazolone (MIT) simultaneously, with removal efficiencies above 80% within 20 min. The photocatalytic degradation of both CMIT and MIT could be modeled using a pseudo-first-order rate equation. The photocatalytic degradation rates of CMIT and MIT under LED280 illumination were higher than under LED310 or LED360 illumination. At concentrations below 100 mg/L, the degradation rate of CMIT and MIT under LED illumination significantly increased with increasing catalyst dosage. Additionally, the effects of the chloride ion concentration, alkalinity and dissolved organic matter on the photocatalytic degradation reaction were also investigated. The $\cdot\text{OH}$ free radicals were determined to play the primary role in the photocatalytic degradation reaction, with a degradation contribution of >95%. The photocatalytic degradation of CMIT and MIT mainly occurred via oxidation, hydrolysis, and chain growth reactions. Finally, the possible photocatalytic degradation pathways of CMIT and MIT over LED/P25 are proposed.

© Higher Education Press 2020

1 Introduction

Kathon is a mixture of methylisothiazolone (MIT) and 5-chloro-2-methyl-4-isothiazolin-3-one (CMIT), and one of the most widely used non-oxidative biocides in wastewater treatment. During reverse osmosis (RO) treatment, Kathon

is widely used to prevent the membrane system from microbial fouling. However, Kathon has been reported to cause human skin allergies (Collier et al., 1990; Richard et al., 1997) and is also regarded as a potential neurotoxin (He et al., 2006; Chen et al., 2016), therefore, methods for Kathon degradation are necessary. In previous studies, it was found that the degradation of Kathon takes a long time, with less than 75% of MIT being degraded using a natural biological system after 96 h (Han et al., 2011), while it took 5 h for CMIT to be removed via electrochemical methods.

✉ Corresponding authors

E-mail: zm-wang@aist.go.jp (Z. Wang); wuqianyuan@sz.tsinghua.edu.cn (Q. Wu)

Among the various available detoxification techniques, photocatalytic decomposition is a feasible one that can be employed to treat water containing non-biodegradable and recalcitrant organic pollutants and have merits over other techniques in safety, effectiveness, and environmental friendliness (Zhang et al., 2018; Li et al., 2019; Mao et al., 2020; Wu et al., 2020). Over the last years, photocatalytic decomposition has emerged as a promising method for the removal of pollutants such as pharmaceuticals, personal care products, and volatile organic compounds. Titanium dioxide (TiO_2) of rich resource, good stability, low cost, and nontoxicity is a representative photocatalyst and show high performance for the photocatalytic decomposition of pollutants such as phenol, tamiflu, dyes, and various kinds of antibiotics and pesticides (Elmolla and Chaudhuri, 2010; Wang et al., 2015). As a well-known commercial TiO_2 , P25 can drive high-efficiency photocatalysis due to its unique mixed anatase and rutile crystal phases and its further modification or hybridization with other materials, e.g., reduced graphene oxide, can achieve even more enhanced or visible light responsive photocatalytic effect (Wang et al., 2018). Because of the great band gap energy (3.0–3.2 eV), UV (< 400 nm) excitation is a prerequisite to activate photocatalysis by TiO_2 , which were usually performed by using mercury lamps, black light tube, or sterilized lamp as a light source (Chen et al., 2018; Ismail et al., 2018). Compared with the ordinary light sources, the Hg-free nontoxic UV light-emitting diodes (LED) is the recently developed energy-saving light sources whose wavelength is available across the UV-A, B, C ranges and their advantages in compact size, stable structure, and shape designing flexibility provide opportunities for sophisticated reactor designs in practical photocatalytic processes. So far photocatalytic oxidation using a UV-LED light source has not yet been applied to the treatment of isothiazolone in concentrate water of a reverse osmosis membrane system.

Herein, P25 was used for the photocatalytic degradation of CMIT and MIT using UV-LED light with different wavelengths (UV-A, B, C) as the light sources. The effects of the water properties, such as the pH, chloride ion concentration, alkalinity, and natural organic matter (NOM) were investigated. It was found that the hydroxyl radical was mainly responsible for the photocatalytic oxidation of CMIT and MIT. Finally, the probable pathways for CMIT and MIT degradation are proposed.

2 Experimental

2.1 Chemicals

Sodium chloride (NaCl), sodium bicarbonate (NaHCO_3), sodium dihydrogen phosphate (NaH_2PO_4), sodium hydroxide (NaOH), and tertiary butyl alcohol (tBA) for the photocatalytic degradation reaction were all analytical

reagent grade. Methanol of the special grade for HPLC analysis was used. Natural organic compounds, Kathon CG, and CMIT (99%) were purchased from the international humus association, Maya Reagent (Aladdin, China), Dr. Ehrenstorfer (Augsburg, Germany), respectively, and MIT (95%) was obtained from J&K Scientific, and CMIT (99%). P25 (80% anatase and 20% rutile) was provided by Evonik Degussa Ltd. All the chemicals were used without any further purification. Ultra-pure water was used in all the degradation reactions and was supplied by a Milli-Q system (Millipore, Massachusetts, USA).

2.2 Photocatalytic experiments

The CMIT and MIT degradation experiments were performed using a home-built quasi-parallel beam LED photocatalytic device. The reaction solution was accommodated in an unsealed round-bottom flask (50 mL) immersed in a water bath whose temperature was maintained to be 298 K. LEDs with wavelengths of 280 nm, 310 nm, and 360 nm were selected as the experimental light sources. In a typical procedure, the P25 catalyst powder was added to a 50 mL solution containing 1 mg/L CMIT or 0.33 mg/L MIT at a given pH value which was adjusted using NaOH and a 5 mmol/L phosphate buffer solution. Depending on the experimental requirements, inorganic anions (Cl^- from NaCl , HCO_3^- from NaHCO_3 for alkalinity), tBA, or natural organic matter were added to the reaction solution. Before the reaction, the catalyst-contained solution was ultrasonicated for 3 min and stirred for 10 min at 400 r/min. The pretreatment can break up any agglomerate so as to ensure uniform dispersion of the catalyst in the solution. Then, the pretreated solution was put underneath the light source and photocatalytic degradation of CMIT or MIT was made upon LED illumination. A 1 mL aliquot of solution was sampled after 0, 1, 2, 4, 7, and 10 min LED illumination and a 0.22 μm polyethersulfone membrane filter was used to remove the catalyst powder from the solutions. The experiments were carried out in triplicate and the results were averaged. Dark experiments which allowed adsorption equilibrium for 1 h without LED illumination were performed to confirm the adsorption property of CMIT and MIT on P25.

2.3 Analytical methods

The concentration of contaminants in the samples was determined via reversed-phase high-performance liquid chromatography (HPLC) using a C18 column. The mobile phase consisted of 50/50% methanol and ultrapure water. The flow rate and injection volume were 0.6 mL/min and 20 μL , respectively. The column temperature was 313 K and the detection wavelength was 273 nm.

The intermediate products generated during the photocatalytic degradation of CMIT and MIT were identified by

a quadrupole time-of-flight mass spectrometer (QTOF), which was equipped with an Agilent 1200-type HPLC apparatus.

The iodometric method was used to analyze the LED light intensity in this work whose detailed procedure was shown in supporting information (Text S1). The light intensities for LED280, LED310, and LED360 were calculated to be 1.37 mW/cm², 1.67 mW/cm², and 3.49 mW/cm², respectively.

3 Results and discussion

3.1 Photocatalytic degradation of CMIT and MIT

In this study, P25 was used as the photocatalyst to degrade CMIT and MIT. Experiments in dark condition confirmed that P25 shows almost no adsorption toward CMIT and MIT and then the effects of adsorption were not considered in subsequent experiments. The degradation efficiencies of CMIT and MIT by photolysis (the LED lights alone) and photocatalysis (the LED lights in coexistence with P25) were studied under illuminations of LED lights of three different wavelengths (360 nm, 310 nm, 280 nm) dubbed by LED360, LED310, and LED280, respectively. As shown in Fig. 1, CMIT and MIT could only be removed by photolysis under illumination of LED280, and their removal ratios reach 18.5% and 27.4%, respectively, after 10 min of illumination. To the contrast, photocatalytic oxidation by P25 under the illumination of the LED lights significantly increased the removal efficiency of CMIT and MIT. 83.8%, 84.1%, and 99.7% of CMIT and 85.5%, 85.0%, and 100% of MIT were removed by LED280, LED310, and LED360, respectively, after 10 min of illumination. The time courses of concentration changes of CMIT and MIT during the photocatalytic processes were curve-fitted according to the following pseudo-first-order equation:

$$\ln(C_t/C_0) = k_1 t \quad (1)$$

where C_0 and C_t are the concentrations of the initial time and after a time interval t , respectively, and k_1 is the first order rate constant. All the fitted curves showed a linearity with a regression coefficient over 0.95 (Fig. S1), indicating that the photocatalytic degradation processes obey the first order kinetics. The k_1 values were calculated to be 0.173, 0.181, and 0.328 min⁻¹ for CMIT, and 0.180, 0.186, and 0.270 min⁻¹ for MIT under illuminations of LED280, LED310, and LED360, respectively. The results demonstrated that CMIT and MIT show no significant difference in photodegradation rate under illumination of each LED UV light source.

The light intensity is an important factor affecting the quantum efficiency and pollutant removal efficiency during the photocatalytic oxidation of organic pollutants.

Because the LED light sources generate different illumination intensities, comparison among the applied LED light sources based on illumination intensity becomes an issue to be considered. As shown in Fig. 1(a,b), when the photodegradation processes are expressed with light dose as the abscissa, the LED280 illuminating the least light intensity appeared to be the most effective light source, becoming to excite a faster degrading reaction toward both CMIT and MIT as compared to the other two light sources. Thus, consideration of the photodegradation reaction based on light intensity is meaningful and an E_p -reduced reaction rate constant, $k_F = k_1/E_p$, was defined and used in the following discussion. From Fig. 1, the k_F values under the illumination of LED280 were calculated to be 0.127 and 0.131 cm²/(mW·min), respectively, which were slightly higher than those under the illumination of LED310 (0.108 and 0.111 cm²/(mW·min) for CMIT and MIT, respectively), and greatly higher than those under the illumination of LED360 (0.094 and 0.077 cm²/(mW·min) for CMIT and MIT, respectively). Both CMIT and MIT have a N-S heterocyclic structure whose characteristic absorption appears at 273 nm, meaning that the two molecules can strongly absorb UV in the wavelength range of 250–300 nm. Hence, UV absorption upon illumination of LED280 can photolyze CMIT and MIT (Fig. 1) through breaking the N-S bond of the five-membered heterocyclic ring in their structure (Sakkas et al., 2002). As the result, the CMIT and MIT molecules are easier to be excited or unstabilized by the LED light with a shorter wavelength so that they can be more easily attacked by free radicals such as ·OH and are effectively decomposed in the photocatalysis processes.

3.2 Effect of photocatalyst dosage

The photodegradation processes of CMIT and MIT under different catalyst dosages followed pseudo-first-order reaction kinetics, from which the E_p -reduced reaction rate constants (k_F) were calculated. Figure 2(a, b) compares the effect of catalyst dosage on photocatalytic degradation of CMIT and MIT based on the k_F values. It is obvious that P25 dosage plays an important role in the LED-excited photocatalytic degradation of CMIT and MIT. In all the cases, the k_F values showed a peak-shape change with photocatalyst dosage, reaching the maximum when photocatalyst dosage is 100 mg/L, although the change of k_F value appears to be more significant in the case of LED310 as compared to those of LED280 and LED360. After exposure of the catalyst to LED illumination, a large amount of active free radicals was generated on the surface, which can attack and degrade the target pollutant on the catalyst surface. The increased catalyst dosage provides increased numbers of active sites to generate active radicals which attend the degradation reaction of CMIT and MIT to increase their degradation rate. On the

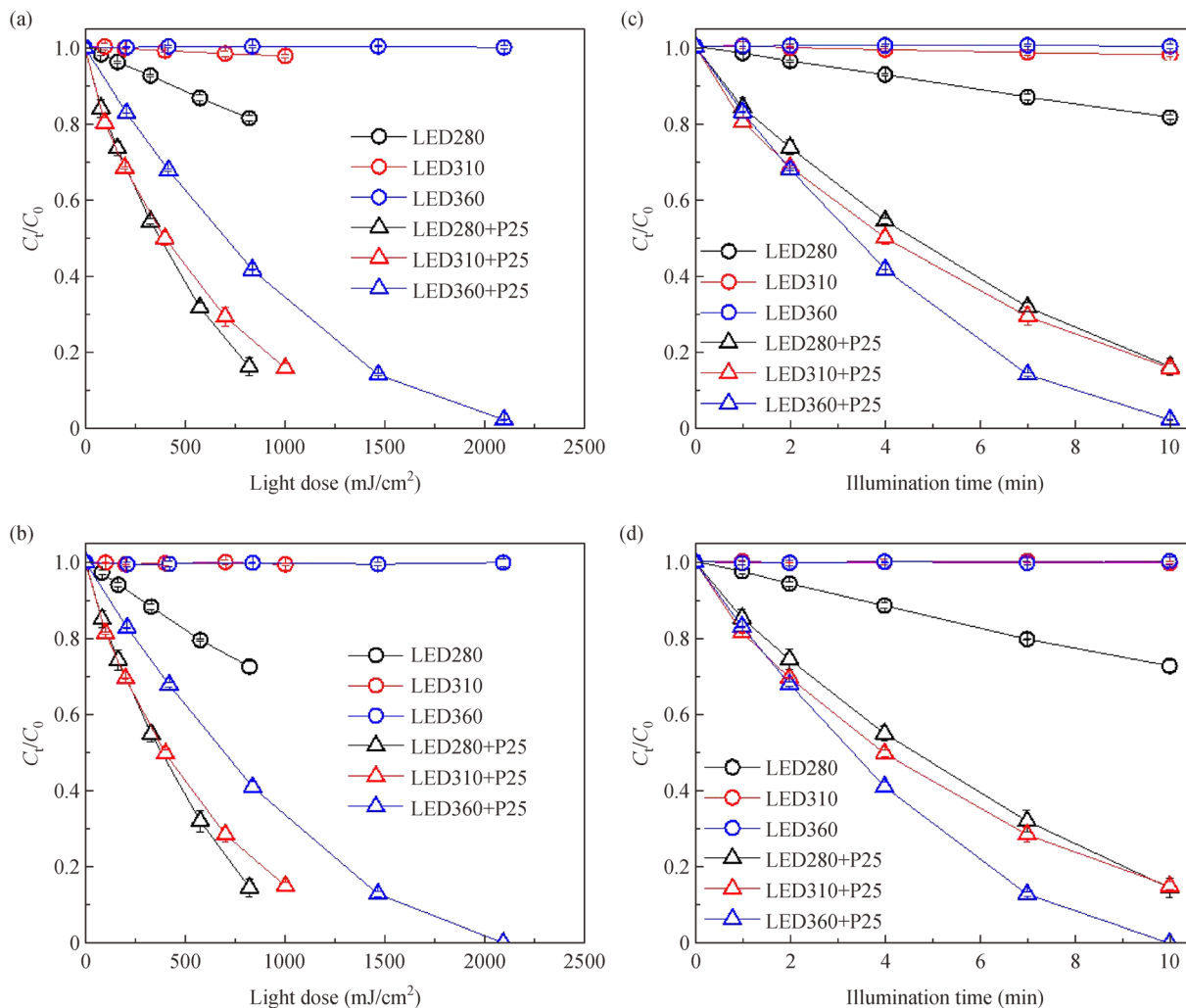


Fig. 1 Degradation of (a, c) CMIT and (b, d) MIT by photolysis (LED alone) and UV-LED photocatalysis over P25. Initial CMIT and MIT concentration were 1 mg/L and 0.33 mg/L respectively, P25 dosage = 200 mg/L, and pH = 7.

other hand, overdose of photocatalyst causes a light-shielding effect, that is, light scattering due to photocatalyst powders makes it difficult for LED light to penetrate into the inside of the solution, particularly, near the bottom of the reactor. Hence, 100 mg/L is the optimum catalyst dosage as the result of trade-off of the effect of increased active sites and the light-shielding effect. In the following condition examinations, 50 mg/L instead of 100 mg/L dosage was chosen to assure sufficient penetration of LED light into the reaction solutions.

3.3 Effect of water quality

The quality of concentrated water in a reverse osmosis membrane system is complex and is possible to influence the photodegradation properties of CMIT and MIT. In this study, the effects of pH and coexisting components such as chloride ions, alkalinity, and natural organic matter were investigated.

3.3.1 Effect of pH

Figure 3 shows the changes of k_F values at different pH values. It is clear that photocatalytic degradation of CMIT and MIT under illuminations of different LED light sources was markedly affected by the pH value and the k_F values were significantly increased (by 5.42, 4.36, and 4.38 times for CMIT and 5.25, 5.59, and 4.81 times for MIT by illuminations of LED280, LED310, and LED360, respectively) with the pH increasing from 5 to 9, although those of CMIT and MIT for LED360 showed a smaller increase (12% and 28%, respectively) in the pH range of 7 to 9. Because CMIT ($pK_a = -4.06$) and MIT ($pK_a = -2.03$) have heteroatoms such as N and O in their structures whose lone pair electrons tend to transfer to protons, they are more easily protonated in acid condition (pH = 5). Under acidic conditions, the surface of P25 (isoelectric point (IEP) = 6.3 (Suttiponparmit et al., 2011)) is positively charged by adsorbing protons, which repels the adsorption

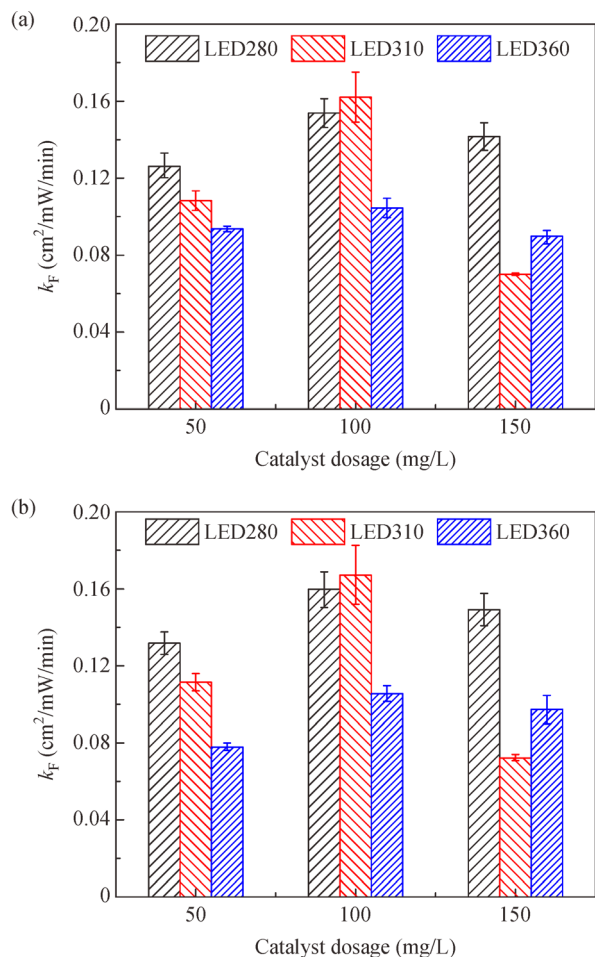


Fig. 2 Light dose-based first-order kinetics rate constant of CMIT (a) and MIT (b) in photocatalytic degradation over P25 of different dosage under illuminations of LED280, LED310, and LED360. Initial CMIT and MIT concentration were 1 mg/L and 0.33 mg/L respectively, and pH = 7.

of CMIT and MIT so as to disadvantage their photodegradation. As the P25 surface becomes negatively charged under neutral or alkaline conditions ($\text{pH} \geq 7$), CMIT and MIT molecules becomes more easily concentrated on the catalyst surface to react with the free $\cdot\text{OH}$ radicals of strong oxidizing power generated there. As the result, the degradation rates at neutral or alkaline conditions were significantly increased when compared with those under acidic condition. Because most RO concentrated water is known to be weakly alkaline, a favorable pollutant removal efficiency can be expected for the P25-driven photocatalytic processes with the LED light sources.

3.3.2 Effect of chloride ion

The chloride ion, as the main anion species present in the concentrated water of a reverse osmosis treatment system, was reported to affect the photocatalytic degradation of

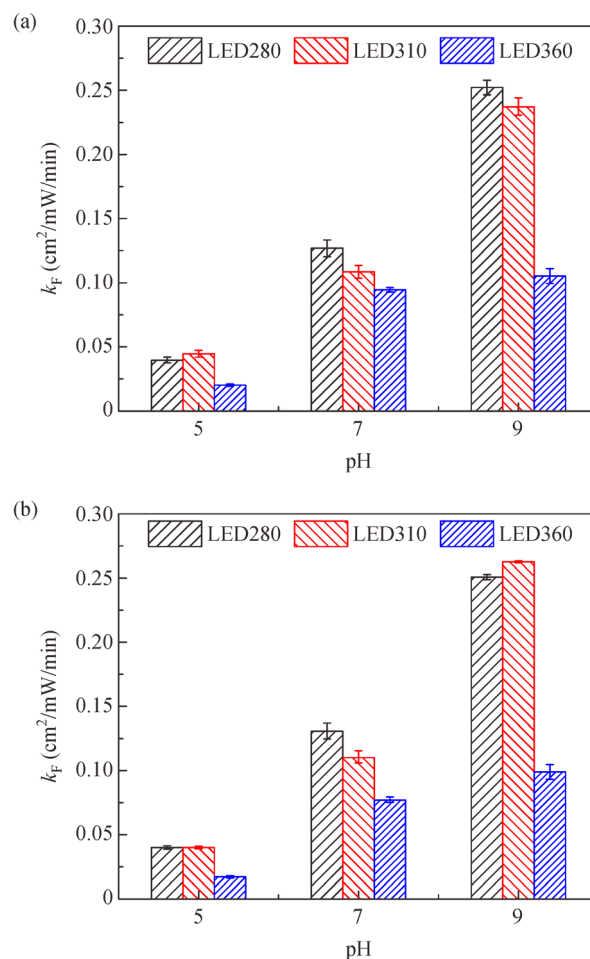


Fig. 3 Light dose-based first-order kinetics rate constant of CMIT (a) and MIT (b) over P25 at different pH values. Initial CMIT and MIT concentration were 1 mg/L and 0.33 mg/L respectively, P25 dosage = 50 mg/L, and pH = 7.

aromatic organic pollutants (Wang et al., 2000; Piscopo et al., 2002). The photodegradations of CMIT and MIT in coexistence with different chloride ion concentrations were examined and the processes obeyed the pseudo first-order kinetics from which the k_F values were calculated. As shown in Fig. 4, chloride ion exhibits a little inhibitory effect on photocatalytic degradations of CMIT and MIT for the cases of LED280 and LED310 but almost no effect for the case of LED360. The inhibition ratios at 500 mg/L of chloride ion were 12.8% and 9.0%, respectively, for the case of LED280; 9.34% and 7.14%, respectively, for the case of LED310; and both close to zero for the case of LED360. As a free radical quencher, chloride ion can rapidly quench $\cdot\text{OH}$ (rate constant, $k = 4.3 \times 10^9 \text{ L}/(\text{mol}\cdot\text{s})$) and generate chlorine-containing free radicals with weak reactivity (Fang et al., 2014). Previous reports on photocatalytic degradation of 2-chlorophenol and 2-nitrophenol have shown that interaction between chloride ion and photocatalyst is weakened at a pH higher

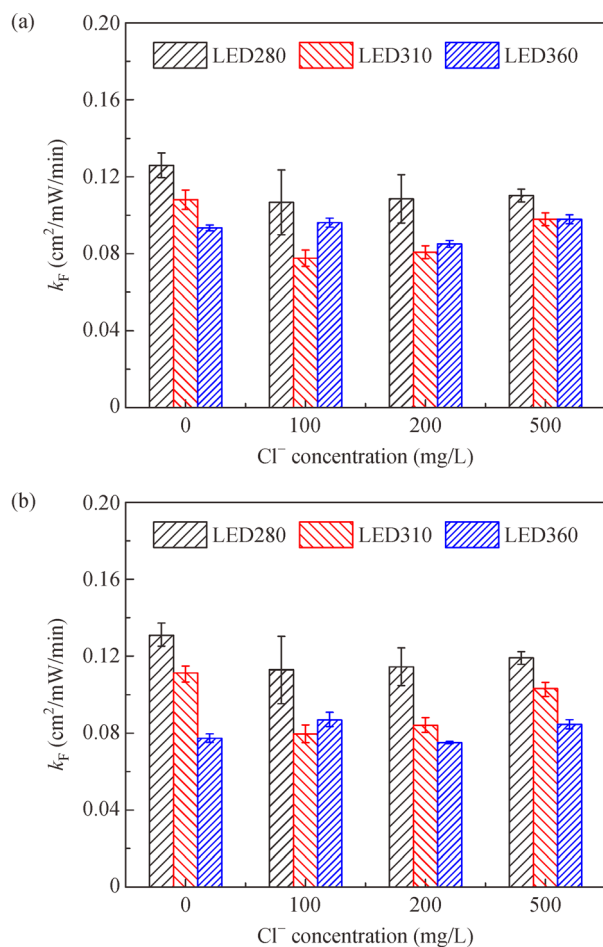


Fig. 4 Light dose-based first-order kinetics rate constant of CMIT (a) and MIT (b) in photocatalytic degradation over P25 under illuminations of LED280, LED310, and LED360 at different chloride ion concentrations. Initial CMIT and MIT concentration were 1 mg/L and 0.33 mg/L respectively, P25 dosage = 50 mg/L, and pH = 7.

than the isoelectric point of the catalyst surface (pH = 6.3 for P25) so that the effect of chloride ion on the photocatalytic degradation efficiency is reduced (Wang et al., 1999). Therefore, the degradation inhibition by chloride ions was not significant at neutral condition.

3.3.3 Effect of alkalinity

Concentrated water in a reverse osmosis treatment system has high alkalinity, mainly in the form of dissolved carbonates and bicarbonates that affect the degradation of organic pollutants via advanced oxidation processes (Liu et al., 2015; Sultan et al., 2016). Figure 5 shows the effect of alkalinity on the photocatalytic degradation of CMIT and MIT in the cases of various LED light sources. The results show that the photodegradation rates of CMIT and MIT were almost unchanged for the case of LED280 which can induce a stronger photocatalysis, but slightly increased

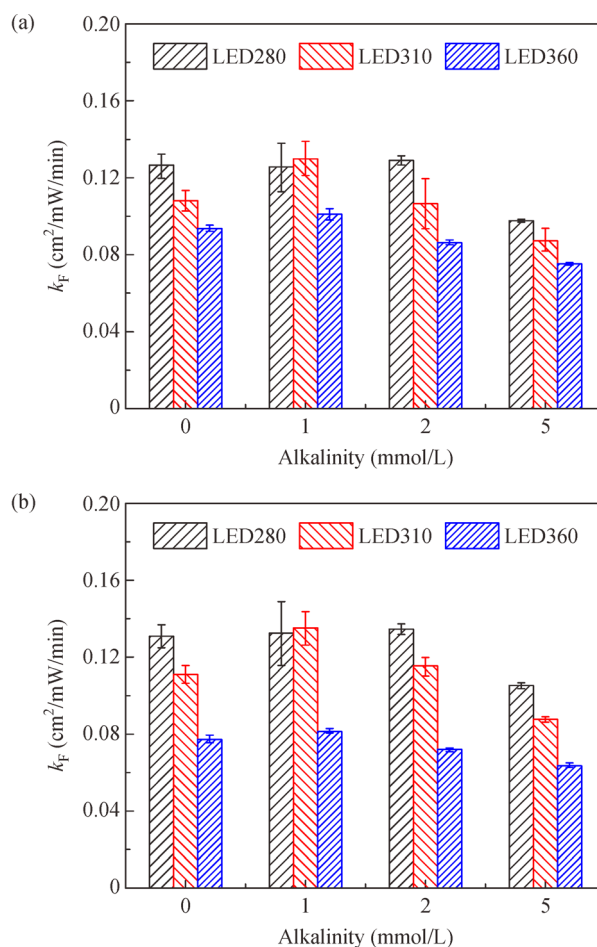


Fig. 5 Light dose-based first-order kinetics rate constant of CMIT (a) and MIT (b) in photocatalytic degradation over P25 under illuminations of LED280, LED310, and LED360 at different alkalinity, initial CMIT and MIT concentration were 1 mg/L and 0.33 mg/L respectively, P25 dosage = 50 mg/L, and pH = 7.

for those cases of LED310 and LED360 at low alkalinity conditions. However, a little decrease in K_F value was observed for all the light source cases at very high alkalinity (not less than 5 mmol/L). It was found that carbonate and bicarbonate ions could promote the degradation of methylene blue although they are considered to be the scavengers of the reactive $\cdot\text{OH}$ radical to form the less reactive $\text{CO}_3^{\cdot-}$ radical ($k = 2 \times 10^8 \text{ L}/(\text{mol}\cdot\text{s})$) (Buxton et al., 1988; Minero et al., 2008). The promotion effect was attributed to the less radical-radical recombination extent of the less reactive $\text{CO}_3^{\cdot-}$ radical as compared to that of the $\cdot\text{OH}$ radical, meaning that the $\text{CO}_3^{\cdot-}$ radical can have more opportunity to contact and react with the target substrates. Hence, similar promotion effect occurs on the surface of the P25 photocatalyst for the light source LED310 and LED360, which results in the enhanced degradation of CMIT and MIT at an appropriate alkalinity. On the other hand, salting-out effect at the condition of

excess alkalinity may increase the difficulty of the catalyst to adsorb CMIT or MIT molecules and thus reduce their probability to react with free radicals generated on the catalyst surface. This accounts for the decreased photodegradation rates of CMIT and MIT at the condition of very high alkalinity (≥ 5 mmol/L).

3.3.4 Effect of SRNOM

A variety of dissolved organics with different molecular structures are present in the concentrated water of a reverse osmosis treatment system which can compete with the target substrates in photocatalytic reactions. Here the typical dissolved natural organic matter from the Suwannee river (SRNOM) was mixed in the CMIT and MIT solutions to examine its influence on photocatalytic degradation of CMIT and MIT. Figure 6 shows that SRNOM significantly inhibited the degradation of CMIT and MIT in the LED/P25 photocatalytic oxidation

processes and the degradation rate constants of CMIT and MIT were progressively decreased with increasing the SRNOM concentration. With the SRNOM concentration increasing to 10 mg-c/L, the k_F values were decreased by 51.9%, 58.9%, and 72.4% for CMIT, and by 52.6%, 59.7%, and 66.4% for MIT for the cases of LED280, LED310, and LED360, respectively. Because of the low reaction selectivity of free radicals toward organic substrates, competition between SRNOM and CMIT or MIT happens to decrease the availability of the $\cdot\text{OH}$ radicals participating in the degradation reaction of CMIT and MIT. This results in the decreased CMIT and MIT degradation rates. In addition, SRNOM can absorb the LED light to the extent to decrease the light intensity reaching the photocatalyst and thus reduce the generation rate of active radicals.

3.4 Removal mechanism of isothiazolinone

3.4.1 Effect of tBA

tBA is generally used as an $\cdot\text{OH}$ radical scavenger because of its fast reaction rate constant of 1.9×10^8 L/(mol \cdot s) with $\cdot\text{OH}$ (Doorslaer et al., 2013). Figure S2 shows the effect of tBA in a concentration of 10 mmol/L on the photocatalytic degradation of CMIT and MIT at different pH values for the LED/P25 systems. Ten mmol/L can be considered as the concentration of tBA which completely quenches the $\cdot\text{OH}$ radicals in the reaction system based on the fast reaction rate constant of tBA with \cdot . The results showed that photocatalytic degradations of CMIT and MIT were almost completely inhibited after addition of 10 mmol/L tBA, indicative of the major contribution of $\cdot\text{OH}$ in the photocatalytic reactions. The inhibition ratio due to addition of tBA, α , defined as the difference of k_F values without and with tBA addition divided by the k_F value without tBA, were calculated and shown in Table 1. From Table 1, the inhibition ratio exceeded 95% for the cases of LED310 and LED360 at all the pH conditions and for the case of LED280 at the neutral and basic conditions, implying that $\cdot\text{OH}$ is almost completely responsible for the photocatalytic degradation of CMIT and MIT at these conditions. On the other hand, the inhibition ratios in acid condition (pH = 5) were lowered to 87.4% and 82.5% for CMIT and MIT, respectively, for the case of LED280 as compared to the above cases. This may suggest a more evident contribution of direct decomposition (photolysis

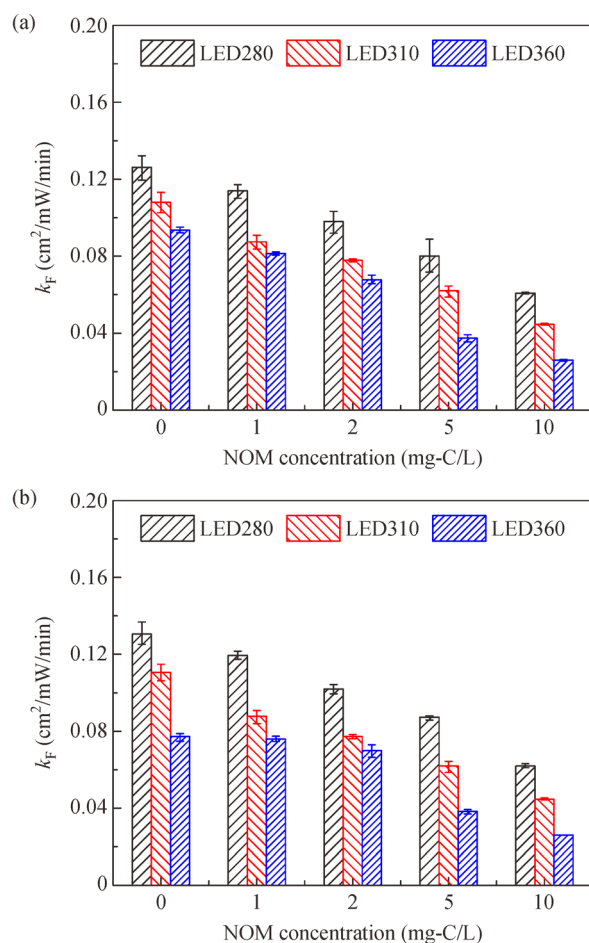


Fig. 6 Light dose-based first-order kinetics rate constant of CMIT (a) and MIT (b) in photocatalytic degradation over P25 under illuminations of LED280, LED310, and LED360 at different NOM concentrations. Initial CMIT and MIT concentration were 1 mg/L and 0.33 mg/L respectively, P25 dosage = 50 mg/L, and pH = 7.

Table 1 Inhibition ratio (α) of tBA toward photodegradation of CMIT and MIT at different pH values

pH	α (%) CMIT			α (%) MIT		
	LED280	LED310	LED360	LED280	LED310	LED360
5	87.4	100	100	82.5	100	100
7	95.4	98.9	98.9	93.9	97.9	98.3
9	98.6	99.2	97.7	96.4	98.5	96.9

through UV absorption) of CMIT and MIT by LED280 at the acidic condition where the decreased adsorption of CMIT and MIT comparatively weakens photocatalysis on the photocatalyst surface.

3.4.2 Transformation products and degradation pathway

The detailed photocatalytic degradation processes of CMIT and MIT were further analyzed with the QTOF-MS technique. Four main degradation products were identified for CMIT after photocatalytic reaction, which were P114 (m/z $[M + H]^+ = 114$), P136 (m/z $[M + Na]^+ = 136$), P198 (m/z $[M-H]^+ = 198$), and P200 (m/z $[M-H]^+ = 200$). To the contrast, only three degradation products were observed for MIT, which were P114 (m/z $[M + H]^+ = 114$), P136 (m/z $[M + Na]^+ = 136$), and P164 (m/z $[M-H]^+ = 164$). The possible intermediate structures were then proposed according to the m/z numbers and shown in Tables 2 and 3 for CMIT and MIT, respectively. Figure 7 shows the changes in response intensities of these degradation products of CMIT and MIT during photocatalysis under illuminations of different LED light sources, which are correspondingly related to the changes in concentrations of such species. It is clear that P114 is the major photodegradation product of both CMIT and MIT for the light sources LED280 and LED310 with shorter wavelength (stronger excitation energy). The species other than P114 (P136, P198, and P200 for CMIT and, P136 and P200 for MIT) had a lower response intensity with some of these species showing a peak change in intensity with the increase of light dose for the two light sources. On the other hand, the response intensities of P198 for CMIT and P164 for MIT were more evident than those of P114 for the light source LED360, indicating that a different photodegradation behavior may occur for LED 360 as compared to the cases of LED280 and LED310.

From the above results, the possible reaction pathways for the photocatalytic oxidation of CMIT and MIT were proposed and schematically depicted in Fig. 8. For CMIT (Fig. 8 (a)), it is inferred that the $\cdot OH$ radical first attacks the N-S bond in its structure because the sulfur atom containing two lone pair electrons can be more easily oxidized by the electrophilic $\cdot OH$. Then photocatalytic process proceeds via either the oxidization or the hydrolysis mechanism to form the P198 and P200 species. Further hydrolysis of these species can remove the terminal sulfate and finally forms the P114 and P136 species through a chain growth mechanism. The chain growth phenomenon which causes the increase in carbon chain length of the degraded products is similar to that observed during the ozone oxidation of isothiazolinone. It is resulted from the reaction of the photodegraded species with carbon-containing free radicals generated during the photocatalysis (Li et al., 2016; Ye et al., 2019).

For MIT (Fig. 8 (b)), the degradation pathway is similar to that of CMIT but becomes simpler because of no involvement of Cl atom in the reactions. The N-S bond in MIT is first attacked by the $\cdot OH$ radical to form the oxidized sulfur group which then is hydrolyzed and further transferred to the P114 and P116 species. It can be considered that dechlorination of CMIT leads to a more complex photodegradation process as compared to MIT. Because the major species are P114 and P136 when photocatalysis proceeds under illuminations of LED280 and LED310, the two light sources tend to excite the chain growth reaction to make those generated species stabilized in the photodegradation solution. To the contrast, P114 and P136 are minor species when photocatalysis is excited by LED360, meaning that LED360 does not favor the chain growth reaction. The more evident P198 (for CMIT) and P164 (for MIT) signals and their hump-shaped change in the response intensities indicate that CMIT and MIT are more likely to be photodegraded or mineralized through

Table 2 Possible intermediate structures during photodegradation of CMIT as identified by LC-QTOF-MS

No.	Experimental m/z	Molecular Formula	Theoretical m/z	Proposed Structure
P 114	114.0913	$C_6H_{12}NO^+$	114.0913	
P 136	136.0723	$C_6H_{11}NONa^+$	136.0733	
P 198	197.9639	$C_4H_5NO_4S(^{35}Cl)^-$	197.9633	
P 200	199.9616	$C_4H_5NO_4S(^{37}Cl)^-$	199.9604	

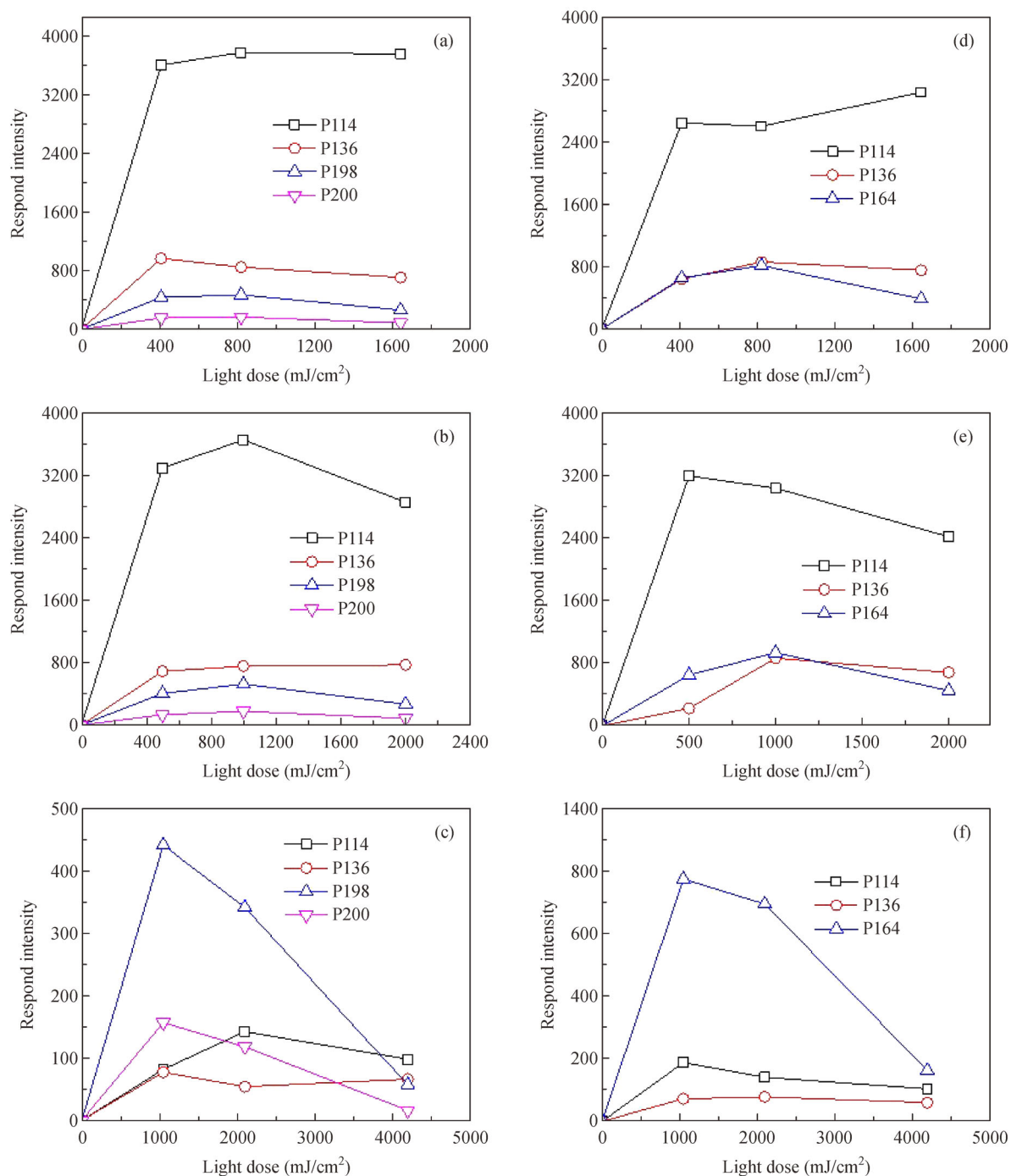


Fig. 7 The change in MASS response intensity of degraded species during photocatalysis of CMIT (a, b, c) and MIT (d, e, f) under illuminations of LED280 (a, d), LED310 (b, e), and LED360 (c, f).

the ordinary photooxidation mechanism when photocatalysis proceeds under illumination of LED360. The difference in photodegradation behavior caused by the type of light sources possibly come from the absorptivity of CMIT and MIT toward LED310 and, particularly, LED280. The molecular absorptivity induces photocatalysis of CMIT and MIT at excited states which leads to the faster degradation rate at the same time to drive a distinct degradation pathway.

4 Conclusions

In this work, CMIT and MIT could be effectively removed via LED/P25 photocatalysis. The removal efficiencies of the LED/P25 photocatalytic system for CMIT and MIT were much higher than those achieved by LED illumination alone. LEDs with different wavelengths were used for the photocatalytic degradation. The shorter LED wavelength light was beneficial for the photocatalytic degrada-

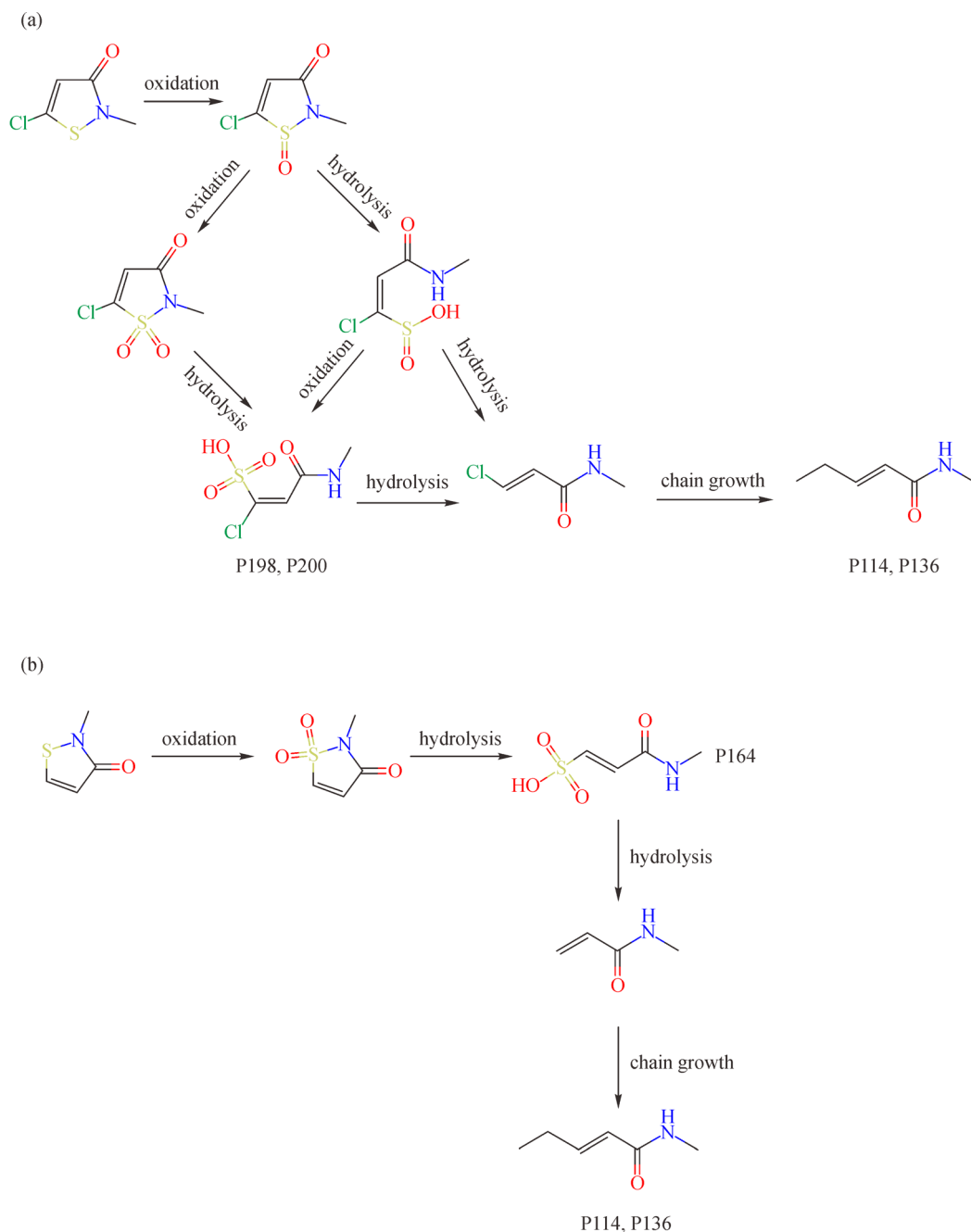
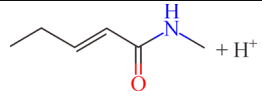
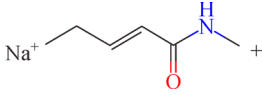
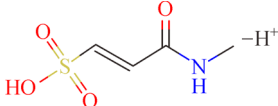


Fig. 8 Possible degradation pathways of CMIT (a) and MIT (b) during the UV-LED/P25 photocatalysis.

tion of CMIT and MIT. When the catalyst dosage was below 100 mg/L, increasing the catalyst dosage could significantly increase the removal efficiencies of CMIT and MIT on LED irradiation. With increasing pH, the photocatalytic degradation rate of CMIT and MIT over P25 slightly increased. A high concentration of chloride ions and a high alkalinity have an inhibitory effect on the LED/P25 photocatalytic degradation of CMIT and MIT, with an inhibition ratio of less than 15%. Dissolved organic matter (natural organic matter) acts as a photomasking agent and a catalyst quencher that significantly inhibited

the degradation of CMIT and MIT by LED/P25 to a degree of 52%–72%. The $\cdot\text{OH}$ was the most active radical species and played the most important role in the photocatalytic degradation process, and its contribution to photodegradation reached more than 95%. On photocatalytic degradation, CMIT and MIT mainly underwent oxidation, hydrolysis, and chain growth reactions. Several intermediate products were detected during the degradation of CMIT and MIT, and their possible respective degradation pathways were proposed.

Table 3 Possible intermediate structures during photodegradation of MIT as identified by LC-QTOF-MS

No.	Experimental m/z	Molecular Formula	Theoretical m/z	Proposed Structure
P 114	114.0913	C ₆ H ₁₂ NO ⁺	114.0913	
P 136	136.0723	C ₆ H ₁₁ NONa ⁺	136.0733	
P 164	164.0006	C ₄ H ₆ NO ₄ S ⁻	164.0012	

Acknowledgements This study was supported by the Major Science and Technology Program for Water Pollution Control and Treatment, China (No. 2017ZX07205001), the Shenzhen Science and Technology Innovation Commission (No. JCYJ20160125095838752), and the Development and Reform Commission of Shenzhen Municipality (Urban Water Recycling and Environment Safety Program). We thank Natasha Lundin, Ph.D., from Liwen Bianji, Edanz Editing China, for editing the English text of a draft of this manuscript.

Electronic Supplementary Material Supplementary material is available in the online version of this article at <https://doi.org/10.1007/s11783-020-1379-x> and is accessible for authorized users.

References

- Buxton G V, Greenstock C L, Helman W P, Ross A B (1988). Critical review of rate constants for reactions of hydrated electrons, hydrogen atoms and hydroxyl radicals ($\cdot\text{OH}/\cdot\text{O}^-$) in aqueous solution. *Journal of Physical and Chemical Reference Data*, 17(2): 513
- Chen L, Zhang W, Ye R, Hu C, Wang Q, Seemann F, Au D W T, Zhou B, Giesy J P, Qian P Y (2016). Chronic exposure of marine medaka (*Oryzias melastigma*) to 4,5-dichloro-2-noctyl-4-isothiazolin-3-one (DCOIT) reveals its mechanism of action in endocrine disruption via the hypothalamus-pituitary-gonadal-liver (HPGL) axis. *Environmental Science & Technology*, 50(8): 4492–4501
- Chen Y, Ye J S, Li C S, Zhou P L, Liu J, Ou H (2018). Degradation of ¹H-benzotriazole by UV/H₂O₂ UV/TiO₂ and ₂: Kinetics, mechanisms, products and toxicology. *Environmental Science and Pollution Research International*, 4: 1282–1295
- Collier P J, Ramsey A, Waigh R D, Douglas K T, Austin P, Gilbert P (1990). Chemical reactivity of some isothiazolone biocides. *Journal of Applied Bacteriology*, 69(4): 578–584
- Van Doorslaer X V, Demeestere K, Heynderickx P M, Caussyn M, Van Langenhove H, Devlieghere F, Vermeulen A, Dewulf J (2013). Heterogeneous photocatalysis of moxifloxacin: Identification of degradation products and determination of residual antibacterial activity. *Applied Catalysis B: Environmental*, 138-139: 333–341
- Elmolla E S, Chaudhuri M (2010). Photocatalytic degradation of amoxicillin, ampicillin and cloxacillin antibiotics in aqueous solution using UV/TiO₂ and UV/H₂O₂/TiO₂ photocatalysis. *Desalination*, 252 (1–3): 46–52
- Fang J, Fu Y, Shang C (2014). The roles of reactive species in micropollutant degradation in the UV/free chlorine system. *Environmental Science & Technology*, 48(3): 1859–1868
- Han W, Chen Y, Wang L, Sun X, Li J (2011). Mechanism and kinetics of electrochemical degradation of isothiazolinones using Ti/SnO₂-Sb/PbO₂ anode. *Desalination*, 276(1–3): 82–88
- He K, Huang J, Lagenaur C F, Aizenman E (2006). Methylisothiazolinone, a neurotoxic biocide, disrupts the association of SRC family tyrosine kinases with focal adhesion kinase in developing cortical neurons. *Journal of Pharmacology and Experimental Therapeutics*, 317(3): 1320–1329
- Ismail L, Ferronato C, Fine L, Jaber F, Chovelon J M (2018). Effect of water constituents on the degradation of sulfaclozine in the three systems: UV/TiO₂, UV/K₂S₂O₈, and UV/TiO₂/K₂S₂O₈. *Environmental Science and Pollution Research International*, 25(3): 2651–2663
- Li A, Wu Q Y, Tian G P, Hu H Y (2016). Effective degradation of methylisothiazolone biocide using ozone: Kinetics, mechanisms, and decreases in toxicity. *Journal of Environmental Management*, 183: 1064–1071
- Li J, Dong X, Zhang G, Cui W, Cen W, Wu S C, Lee, Dong F (2019). Probing ring-opening pathways for efficient photocatalytic toluene decomposition. *Journal of Materials Chemistry. A, Materials for Energy and Sustainability*, 7(7): 3366–3374
- Liu Y, He X, Duan X, Fu Y, Dionysiou D D (2015). Photochemical degradation of oxytetracycline: Influence of pH and role of carbonate radical. *Chemical Engineering Journal*, 276: 113–121
- Mao W, Zhang L X, Wang T Y, Bai Y C, Guan Y T (2021). Fabrication of highly efficient Bi₂WO₆/CuS composite for visible-light photocatalytic removal of organic pollutants and Cr(VI) from wastewater. *Frontiers of Environmental Science and Engineering*, 15, 52
- Minero C, Pellizzari P, Maurino V, Pelizzetti E, Vione D (2008). Enhancement of dye sonochemical degradation by some inorganic anions present in natural waters. *Applied Catalysis B: Environmental*, 77(3–4): 308–316
- Piscopo A, Robert D, Weber J V (2001). Influence of pH and chloride anion on the photocatalytic degradation of organic compounds. *Applied Catalysis B: Environmental*, 35(2): 117–124
- Richard C, Bosquet F, Pilichowski F J (1997). Photocatalytic transformation of aromatic compounds in aqueous zinc oxide suspensions: effect of substrate concentration on the distribution of products. *Journal of Photochemistry and Photobiology A Chemistry*,

- 108(1): 45–49
- Sakkas V A, Konstantinou I K, Albanis T A (2002). Aquatic phototransformation study of the antifouling agent Sea-Nine 211: Identification of byproducts and the reaction pathway by gas chromatography-mass spectroscopy. *Journal of Chromatography A*, 959(1–2): 215–227
- Sultan T, Cho J (2016). Optimization of a UV/H₂O₂ AOP system using scavenger radicals and response surface methodology. *Chemical Engineering Communications*, 203(8): 1093–1104
- Suttiponparnit K, Jiang J K, Sahu M, Suvachittanont S, Charinpanitkul T, Biswas P (2011). Role of surface Area, primary particle size, and crystal phase on titanium dioxide nanoparticle dispersion properties. *Nanoscale Research Letters*, 6: 27–35
- Wang K H, Hsieh Y H, Chou M Y, Chang C Y (1999). Photocatalytic degradation of 2-chloro and 2-nitrophenol by titanium dioxide suspensions in aqueous solution. *Applied Catalysis B: Environmental*, 21(1): 1–8
- Wang K H, Hsieh Y H, Wu C H, Chang C Y (2000). The pH and anion effects on the heterogeneous photocatalytic degradation of o-methylbenzoic acid in TiO₂ aqueous suspension. *Chemosphere*, 40(4): 389–394
- Wang W L, Wu Q Y, Wang Z M, Hu H Y, Negishi N, Torimura M (2015). Photocatalytic degradation of the antiviral drug Tamiflu by UV-A/TiO₂: Kinetics and mechanisms. *Chemosphere*, 131: 41–47
- Wang Z M, Hirotsu T, Wu H, Kanoh H (2018). Advantaging synergy photocatalysis with carbon as a counterpart player of titania. *Chemical Record (New York, N.Y.)*, 18: 1–15
- Wu Q Y, Wang J, Wang Z W, Xu Y L, Xing Z H, Zhang X Y, Guan Y T, Liao G F, Li X Z (2020). High-loaded single Cu atoms decorated on N-doped graphene for boosting Fenton-like catalysis under neutral pH. *Journal of Material Chemistry A*, 8:13685–13693
- Ye B, Chen Z, Li X Z, Liu J N, Wu Q Y, Yang C, Hu H Y, Wang R H (2019). Inhibition of bromate formation by reduced graphene oxide supported cerium dioxide during ozonation of bromide-containing water. *Frontiers of Environmental Science and Engineering*, 13(6): 86–94
- Zhang K, Wang J, Jiang W J, Yao W Q, Yang H P, Zhu Y F (2018). Self-assembled perylene diimide based supramolecular heterojunction with Bi₂WO₆ for efficient visible-light-driven photocatalysis. *Applied Catalysis B: Environmental*, 232: 175–181